

Evaluation of Cambay shale Cambay basin, India using geo-mechanical properties

Priti R. Gangwar · Anirbid Sircar

Received: 8 March 2013 / Accepted: 13 August 2013 / Published online: 25 August 2013
© The Author(s) 2013. This article is published with open access at Springerlink.com

Abstract Shale formations have laminated structures with significant variations in mechanical properties along the orientations of the bedding plane. This results in anisotropy, which is an important issue in exploration. The goal of the study is to analyse the physical properties of two core samples from Cambay basin, Gujarat (phase composition, crystallographic preferred orientation, crystal structure and texture) and to compute the Thomsen parameters using synchrotron X-ray diffraction method. To analyse complicated diffraction images resulting from different clay minerals (illite and smectite, kaolinite, quartz, siderite, feldspar), Rietveld refinement method was used. Our results show that elastic anisotropy resulting from crystallographic preferred orientation of the clay particles can be determined quantitatively. This study also provides a possible way to measure anisotropy mathematically.

Keywords Cambay shale · X-ray synchrotron diffraction method · Rietveld refinement · Thomsen parameters · Velocity anisotropy

Abbreviations

OD	Orientation distribution
TIFF	Tagged image file format
MAUD	Material analysis using diffraction
I/S	Illite and smectite
MRD	Multiples of random distribution

P. R. Gangwar · A. Sircar (✉)
School of Petroleum Technology, Pandit Deendayal Petroleum University, Gandhinagar 382007, India
e-mail: anirbid.sircar@spt.pdpu.ac.in

P. R. Gangwar
e-mail: priti.gangwar15@gmail.com

Introduction

The depleting oilfields across the world have led to an increase in the exploration of unconventional resources of energy. Shale gas is the most promising among the other sources. In India too, energy ‘demand versus supply’ gap has increased the focus on developing shale gas. Higher natural gas prices in the recent years and advances in shale gas producing technologies, namely, hydraulic fracturing and horizontal drilling have made shale gas profitable in recent times.

A number of sedimentary basins in India including Cambay, Assam-Arkana and Damodar have large shale deposits. To achieve a reliable supply of shale gas, Indian companies have already taken an initiative in exploring shale gas prospects.

Shale gas is natural gas that never migrates but remains trapped in the original source rock and adsorbs on the insoluble organic matter. Gas Shales are, therefore, both the source rock as well as the reservoir for the natural gas. They are characterized by ultralow permeability and the micropore spaces that can barely accommodate flow of tiny methane molecules (Sandrea 2012). Shale gas typically is a dry gas composed primarily of methane.

To have a gas producing potential, the shale must possess sufficient organic matter and the lithology should be brittle enough to allow artificial fracturations. A quantitative understanding of the texture and thus the intrinsic contribution of single crystals and their orientation to anisotropy may help us to evaluate the effects of the oriented fracture which may be utilized for fracturing and exploitation of shale gas. All shale gas rocks are intrinsically anisotropic due to the presence of clay minerals; they are typically overpressured due to trap fluids in pores; they contain organic materials; and they have low porosity and

permeability (Sondergeld and Rai 2011). The anisotropy of elasticity mainly depends on preferred orientations of rock forming minerals, single crystal properties, the fracture and pore distribution and pressure–temperature conditions (Hornby et al. 1994). Preferred orientation or texture is caused by slow sedimentation of plate-shaped clay minerals that favours orientation of platelets parallel to the sediment surface. This pattern is modified during compaction and diagenesis (Khan et al. 2011).

In sedimentary terms, shale is a fine-grained clastic rock typically <4 microns in diameter formed by consolidation of silts and clay. Clay minerals are fine grained and poorly crystalline. Conventional analysis with X-ray pole figures gives only limited information. Hard X-ray produced at synchrotron sources provides a new method to investigate weakly scattering materials. Highly focused X-ray beam with short wavelength permits high penetration without major adsorption (Schoenberg and Sayers 1995). Two dimensional detectors, either charge-coupled device cameras or image plates are used to record diffraction images. Shales are polyphase materials with many overlapping reflections. Both quantitative phase and texture analyses are necessary to determine the volume fractions and the orientation distributions (ODs) for each mineral, respectively. The recently developed Rietveld method has emerged as a powerful tool to extract reliable texture information (Reitveld 1969; Wenk et al. 2007).

Our aim is to investigate the shale anisotropy and texture of shale using the Geo-mechanical data. X-ray synchrotron diffraction is used to study the texture of the two shales of Cambay basin, older and younger Cambay shale taken from the Sanand region of the Cambay basin. Rietveld method is used to determine the 3D ODs; from the OD we obtained the polycrystalline elastic tensor by averaging the single crystal elastic properties. From the above studies the compressional and shear wave velocities and their texture-related component, anisotropy, is calculated.

Experiment

Two different shale samples were chosen for the Geo-mechanical analysis from the Sanand field of Cambay basin, Gujarat, India. Cambay shale was deposited during the Eocene time when synrift stage was continuing. The shale is predominantly black to dark grey in colour. The Cambay shale is further divided into older Cambay shale and younger Cambay shale formations. Detailed understanding of Cambay shale is available in the literature (Chowdhary 2004; Biswas 1999; Scarrar et al. 2000). The first one from a higher level is a younger Cambay shale with high density ($\rho = 2.21$ g/cc) and the second one from the lower level older Cambay shale with a low density ($\rho = 2.16$ g/cc).

The samples from the Cambay shale were analysed on a high-energy beam line. The samples were mounted on the metal rod parallel to the vertical axis, y on a Goniometer. Images were recorded using a Mar345 image plate detector as shown in Fig. 1. The intensity variations along the Debye rings immediately reveal the presence of texture. A lanthanum hexaboride powder standard was used to calibrate the sample-to-detector distance and refine instrumental parameters. After recording the above data, images were converted to FIT2D to 16-bit tagged image file format (TIFF) and exported for further processing (Lonardelli et al. 2007).

The TIFF images were entered into the material analysis using diffraction (MAUD) programme, a Rietveld code written in Java (Lutterotti et al. 1997). Using Rietveld refinement method the unknown crystal structure, crystal-lite size and the amount of disorder are determined. Also the quantitative phase analysis is extracted. The refined values are shown in Table 1.

The (100), (010) and (001) pole figures are used for the graphic representation. The aim of this work is to quantify the texture; thus, illite and smectite are treated as a single

Fig. 1 Schematic sketch illustrating an X-ray diffraction experiment. The diffraction pattern is recorded with a 2D detector. (Lonardelli et al. 2007)

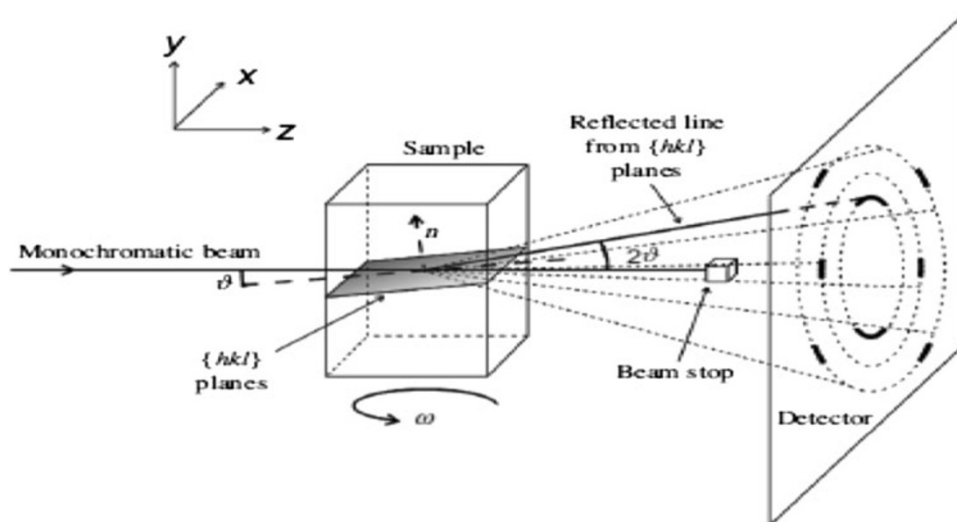


Table 1 Density, anisotropic crystallite size and the quantitative phase information (in weight fraction)

Sample	Density (g/cm ³)	Crystallite size (nm)			Weight fraction (%)					
		100	010	001	I/S	Kaolinite	Quartz	Siderite	Feldspar	
Younger Cambay shale	2.21	I/S	15.2 (8)	14.2 (8)	5.6 (8)	35 (2)	44 (2)	14.2 (1)	4.6 (1)	1.8 (1)
		Ka	21.2 (7)	21.2 (7)	13.2 (7)					
Older Cambay shale	2.16	I/S	22.9 (7)	17.6 (12)	2.9 (2)	32 (2)	38 (2)	11.2 (4)	5.6 (1)	3.5 (1)
		Ka	16.4 (7)	22.9 (8)	10.8 (4)					

The error generated during Rietveld refinement (standard deviation) is shown in the parentheses

mixed layer phase in both samples (I/S), with a 1:1 ratio (50 % illite, 50 % smectite).

Results and discussion

Material analysis using diffraction was used to extract ODs for quartz, feldspar, siderite, I/S and kaolinite and for further processing the data were exported in BEARTEX. The strength of the lattice-preferred orientations (texture strength, F2), the Orientation distribution minimum and maximum, and additional texture information are summarized in Table 2.

For samples, I/S display strong preferred orientation (4.41 and 5.92). Kaolinite is oriented in younger Cambay shale but more or less oriented in older Cambay shale. In Older Cambay shale, Kaolinite distribution for 001 range maximum 1.21 and minimum 0.91 is more oriented; this orientation indicates anisotropy. Quartz, Feldspar and Siderite are randomly oriented, so pole figures for silt components are not shown.

For younger Cambay Shale, (001) pole figures display a maximum concentration of 3.32 multiples of random distribution (MRD). The significant minimum (001) of approximately 0.32 MRD tells us that the significant portion of the crystallites is randomly oriented. The (100) pole

Table 2 Quantitative texture information for OD and pole figures in multiples of random distribution (MRD)

Sample		F2 (min/max)	OD (max/min)	001 (max/min)	100 (max/min)
Younger Cambay shale	I/S	1.32	4.41/0.26	3.32/0.32	1.35/0.62
	Kaolinite	1.22	3.21/0.25	2.63/0.4	1.29/0.61
Older Cambay shale	I/S	1.78	5.92/0.23	4.69/0.23	1.42/0.36
	Kaolinite	1.02	2.26/0.78	1.21/0.91	1.12/0.88

Table 3 Cambay shale Thomsen parameter

Sample	Average		Elastic constants Gpa					Thomsen parameter		
			C ₁₁	C ₃₃	C ₄₄	C ₁₃	C ₆₆	ε	γ	δ
Younger Cambay shale	I/S	Geometric	112.2	103.2	35	37.2	35.7	0.023	0.041	0.005
		Voigt	143.6	122.8	49.2	37.6	43.5	0.044	0.032	0.004
		Reuss	89.2	83.6	26.5	28.3	28.7	0.035	0.013	0.007
	Ka	Geometric	79.2	72.4	24.3	20.1	41.2	0.023	0.021	0.032
		Voigt	121.3	112.5	40.1	34.3	15.3	0.029	0.013	0.031
		Reuss	47.1	45.2	16.6	12.1	15.6	0.021	0.015	0.041
Older Cambay shale	I/S	Geometric	115.8	99.8	30.7	12.1	16.1	0.069	0.016	-0.016
		Voigt	142.9	116.5	29.1	36.2	44.3	0.067	0.017	-0.012
		Reuss	88.4	96.2	17.1	32.2	28.9	0.045	0.017	-0.026
	Ka	Geometric	123.2	102.8	14.7	32.6	34.6	0.032	0.018	-0.012
		Voigt	149.4	138.2	48.8	39.5	17.6	0.012	0.019	-0.013
		Reuss	51.8	124.1	96.2	28.5	27.5	0.015	0.016	-0.018

figures for the I/S displayed no significant concentration, indicating the mineral tend to align in a fibre texture rotating freely around the (001) normal. In younger Cambay Shale, the strong texture for clay minerals, I/S and Kaolinite, is also easily recognized.

In older Cambay Shale, I/S is more strongly aligned than in younger Cambay Shale, with (001) poles having a maximum value of 4.69 MRD. The volume fraction of the randomly oriented crystallites is similar (0.23 MRD). I/S is more textured in Older Cambay Shale than in younger Cambay Shale, although Kaolinite is nearly randomly oriented with a (001) maximum of approximately only 1.21 MRD.

Results for aggregate elastic constants weighted by the OD are shown in Table 3 which shows the Elastic Stiffness of I/S and Kaolinite aggregates using the geometric mean (Geo), Voigt average (upper limit), Reuss average (lower limit) and calculated Thomsen anisotropy parameters. The Voigt and Reuss values provide upper and lower bounds, assuming uniform strain and uniform stress, respectively, throughout the textured aggregate. Geometric mean averages are the intermediate values of Voigt and Reuss. (Matties and Humbert 1993).

Table 3 shows Thompson parameter and elastic constant for both Younger and Older Cambay shale, Thompson parameter ϵ shows P-wave anisotropy in the formation, while γ measures the S-wave anisotropy and δ is totally independent of horizontal velocity which and may be either positive or negative. From the table we can see the presence of P-wave anisotropy in Older Cambay shale. This indicates the velocity in horizontal direction is more than that in vertical direction.

The elastic constants for I/S and kaolinite for younger and older Cambay shale are compared using bar diagrams.

Figures 2, 3, 4 and 5 show that the elastic constants C_{11} , C_{33} and C_{44} have higher values than C_{13} and C_{66} for kaolinite and I/S in both older and younger Cambay shale

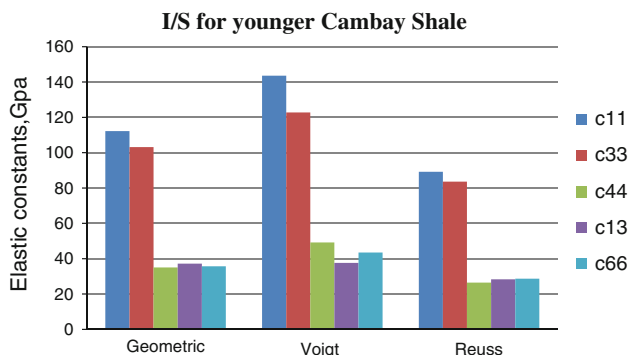


Fig. 2 I/S for Younger Cambay shale versus Voigt, Geometric and Reuss

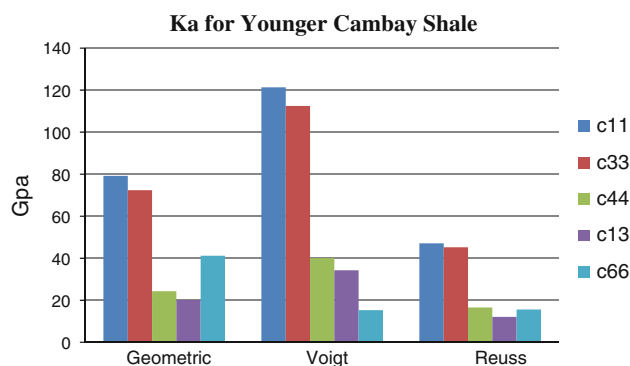


Fig. 3 Average of Kaolinite Younger Cambay shale V_s Voigt, Geometric and Reuss

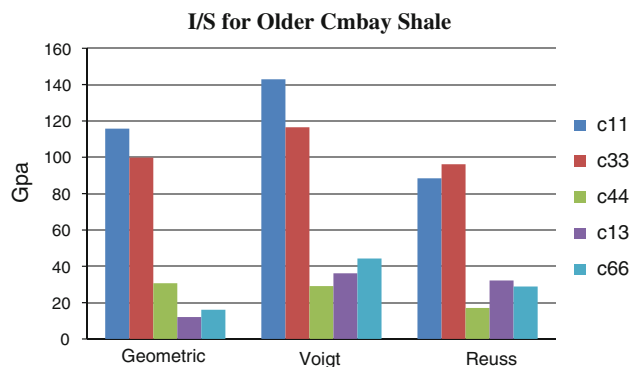


Fig. 4 I/S for Older Cambay shale of Voigt, Geometric and Reuss

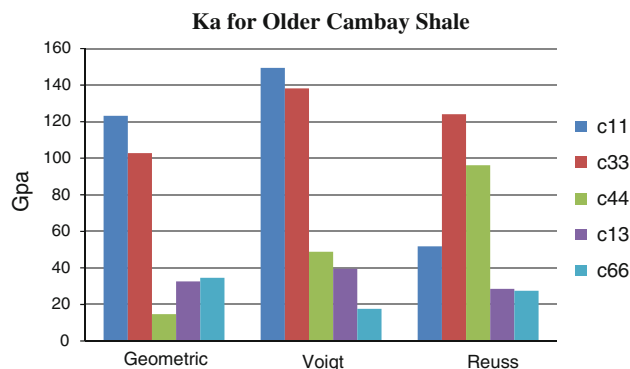


Fig. 5 Average of Kaolinite for Older Cambay shale of Voigt, Geometric and Reuss

which suggests that the compression force is more than the shear force in both the shales (Berryman et al. 1997).

The elastic constants can be utilized to calculate the Thomsen parameters ϵ , γ and δ .

Thomsen parameters are dimensionless combinations of the elastic moduli which characterize transversely isotropic materials. In terms of the components of the elastic stiffness matrix, these parameters are given as,

$$\varepsilon = \frac{C_{11} - C_{33}}{2C_{33}}$$

$$\gamma = \frac{C_{66} - C_{44}}{2C_{44}}$$

and

$$\delta = \frac{(C_{13} + C_{44})^2 - (C_{33} - C_{44})^2}{2C_{33}(C_{33} - C_{44})}$$

where ε and γ represent measurements of anisotropy of P-wave velocity and S-wave velocity, respectively. δ is a parameter that is useful in reflection velocity analyses because it describes weak anisotropy in transversely isotropic media and is almost independent of the horizontal velocities (Thomsen 1986).

Also Young’s modulus, Poisson’s ratio, Bulk modulus and Shear modulus can be evaluated using the following equations from the elastic constants. The Table 4 shows the calculated parameters (Pena 1998).

The equations used are,

$$K = \frac{C_{33}(C_{11} + C_{12}) - 2C_{13}^2}{2C_{33} + C_{11} + C_{12} - 4C_{13}}$$

$$Y_1 = \frac{[C_{33}(C_{11} + C_{12}) - 2C_{13}^2](C_{11} - C_{12})}{C_{33}C_{11} - C_{13}}$$

$$Y_3 = \frac{[C_{33}(C_{11} + C_{12}) - 2C_{13}^2]}{C_{11} + C_{12}}$$

$$v_{31} = \frac{C_{13}}{C_{11} + C_{12}}$$

$$v_{12} = \frac{C_{33}C_{12} - C_{13}^2}{C_{11}C_{33} - C_{13}^2}$$

Figure 6 highlights the variation of vertical and horizontal Poisson’s ratio versus Epsilon. Epsilon is the Thomsen parameter which shows the anisotropy in rocks. The graph shows that the horizontal Poisson’s ratio remains almost the same for given range of Epsilon. But the vertical Poisson’s ratio decreases with Epsilon showing that the strain varies vertically in shale.

Table 4 The calculated results from the elastic constants

Thomsen parameters			Young’s modulus		Poisson’s ratio			Bulk modulus
ε	γ	Δ	Y1	Y3	v_{31}	v_{13}	v_{12}	K_0
0.023	0.041	0.005	80.5561	85.1106	0.2431	0.2605	0.2773	0.3605
0.044	0.032	0.004	107.5705	108.6765	0.1878	0.2017	0.3413	0.3062
0.035	0.013	0.007	65.7834	70.3621	0.2339	0.2440	0.2791	0.3385
0.023	0.021	0.032	67.6966	61.7682	0.2645	0.3107	-0.1193	0.2776
0.029	0.013	0.031	48.3258	101.4010	0.1618	0.0842	0.7239	0.3049
0.021	0.015	0.041	37.6551	40.5521	0.1921	0.1904	0.2887	0.2677
0.069	0.016	-0.016	54.6877	98.3315	0.0607	0.0341	0.7184	0.1212
0.067	0.017	-0.012	108.5545	103.2095	0.1836	0.2091	0.3270	0.3107
0.045	0.017	-0.026	63.9556	78.7741	0.2706	0.2492	0.2554	0.3347
0.032	0.018	-0.012	88.1444	90.8050	0.1840	0.1944	0.3869	0.3171
0.012	0.019	-0.013	56.8954	126.3620	0.1498	0.0728	0.7451	0.2858
0.015	0.016	-0.018	37.8713	90.6741	0.5864	0.2791	-0.2153	0.2297

Fig. 6 Variation of Poisson’s ratio and epsilon

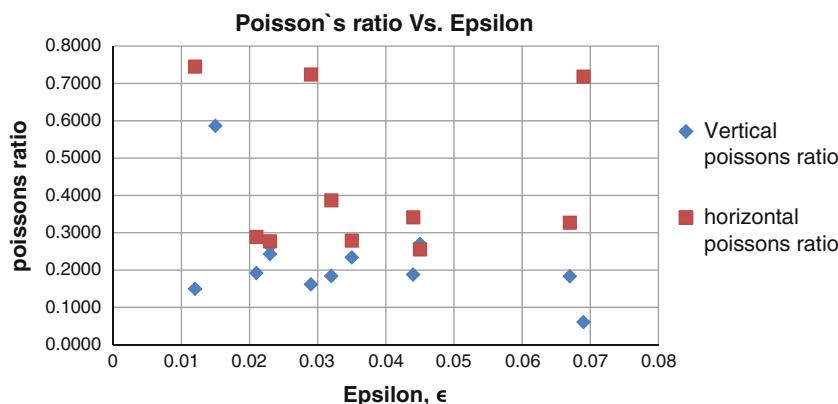


Fig. 7 Variation of Poisson's ratio and gamma

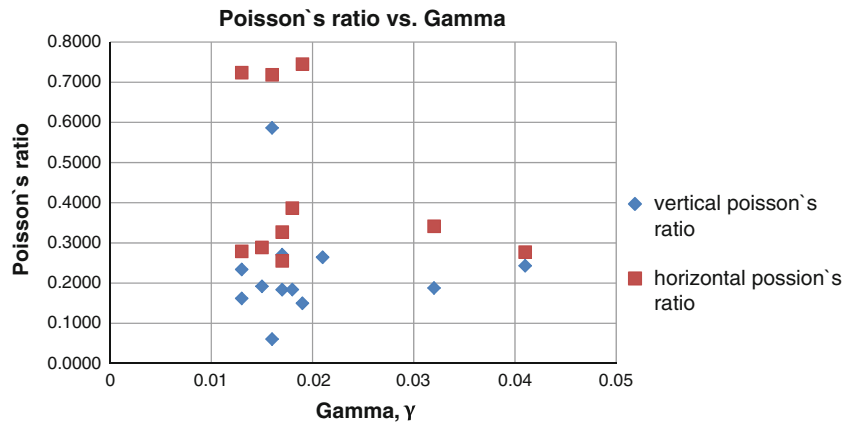
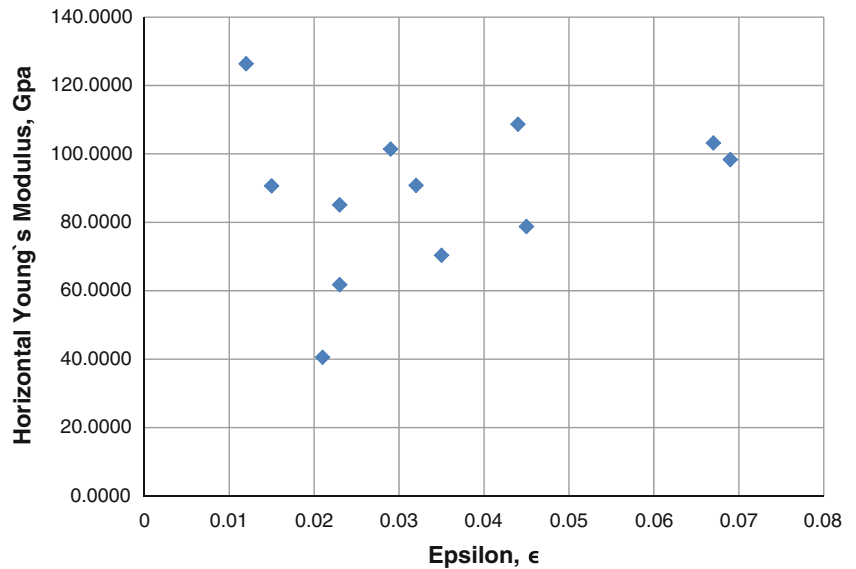


Fig. 8 Horizontal Young's modulus versus epsilon



Gamma, γ shows the anisotropy in the P wave or compressional wave. Figure 7 shows the decrease in Poisson's ratio both in vertical and horizontal directions with Gamma.

Figure 8 demonstrate that the horizontal Young's modulus show very low variation with Epsilon indicating that the shale is isotropic in horizontal direction.

The plot of vertical Young's modulus with Epsilon in Fig. 9 shows the scattered behaviour with three trend lines which depicts multiple Young's modulus values for the sample. This indicates horizontally foliated structure of the shale.

Thomsen parameters are used as a measure of velocity anisotropy. From aggregate elastic constants obtained by geometric mean, we calculated the phase velocity surfaces (V_p , V_{sv} and V_{sh}) from the following equations:

$$\rho V_p^2 = C_{44} + \frac{1}{2}(h \cos^2 \theta + a \sin^2 \theta) + \frac{1}{2} \left[(h \cos^2 \theta + a \sin^2 \theta)^2 - 4(a h - d^2) \cos^2 \theta \sin^2 \theta \right]^{1/2}$$

$$\rho V_{sv}^2 = C_{44} + \frac{1}{2}(h \cos^2 \theta + a \sin^2 \theta) - \frac{1}{2} \left[(h \cos^2 \theta + a \sin^2 \theta)^2 - 4(a h - d^2) \cos^2 \theta \sin^2 \theta \right]^{1/2}$$

$$\rho V_{sh}^2 = C_{44} \cos^2 \theta + C_{66} \sin^2 \theta$$

$$\Delta S = V_{sv} - V_{sh}$$

where,

$$a = C_{11} - C_{44}$$

$$h = C_{33} - C_{44}$$

$$d = C_{13} + C_{44}$$

where θ is the angle measured from the symmetry axis, V_p is the compressional velocity, V_{sv} is the vertically polarized shear wave velocity and V_{sh} is the horizontally polarized shear wave velocity. These velocities are plotted against the angle from the bedding normal symmetric axis in degrees. The variations are shown in Fig. 10 and 11.

Fig. 9 Vertical Young's modulus versus Epsilon

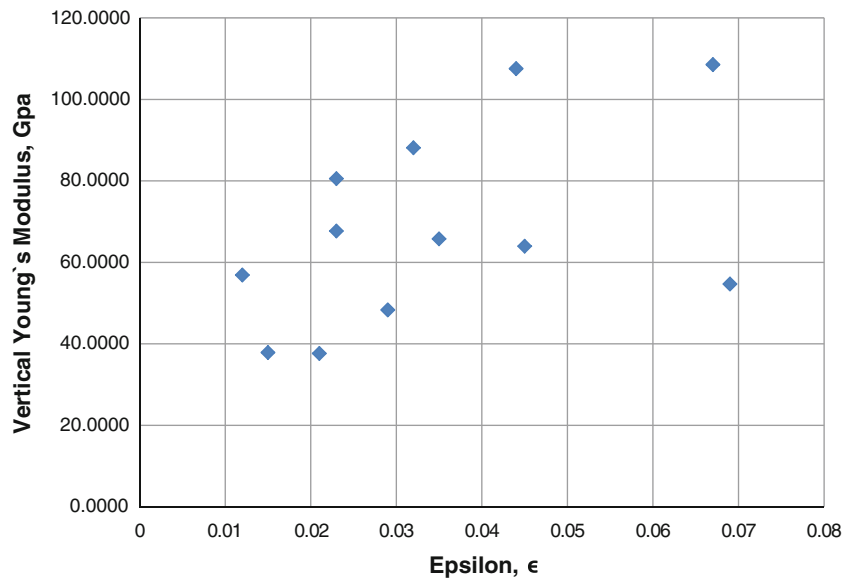
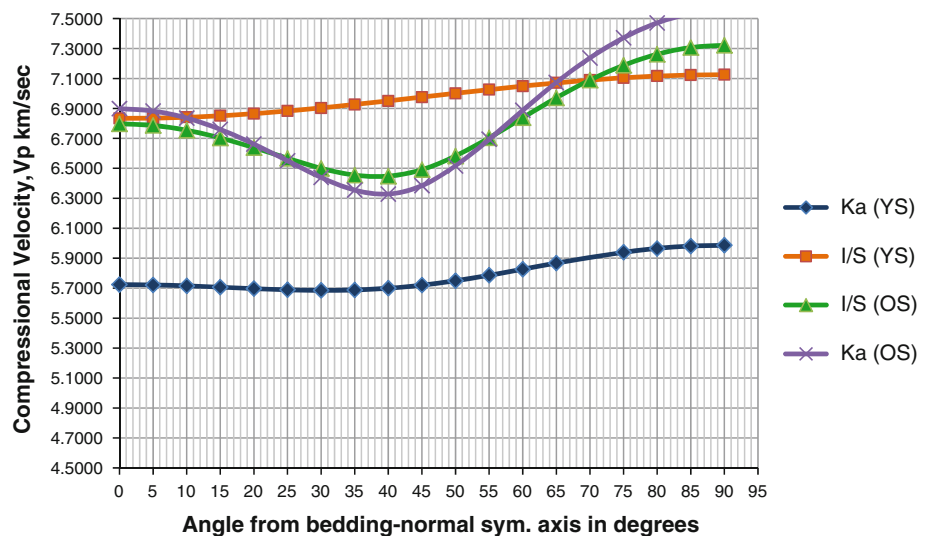


Fig. 10 Calculated seismic P-waves velocity for I/S and Ka (younger and older Cambay shale) versus the angle of the bedding plane

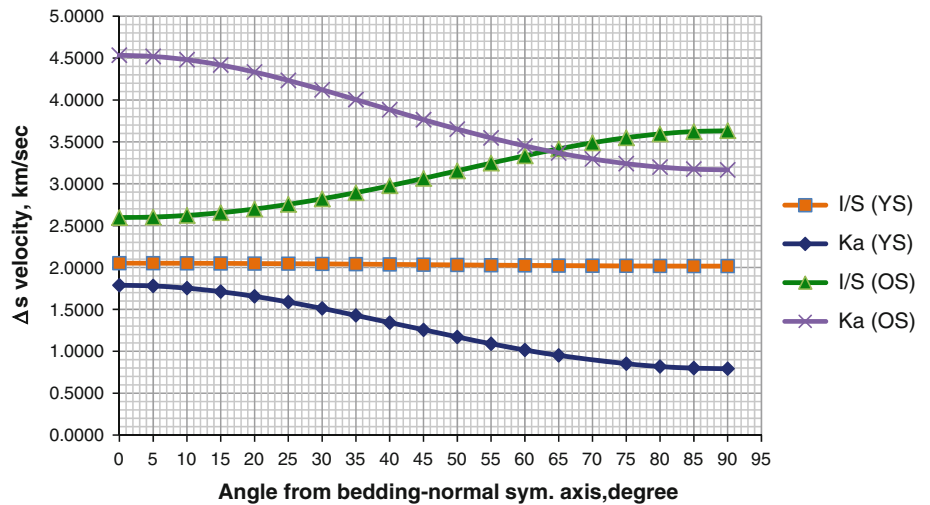


The compressional velocity in younger Cambay shale for Illite and Smectite (I/S), and Kaolinite (Ka) shows slight variation with the angle from the bedding plane with the minimum (5.7 km/s in Ka and 6.83 km/s in I/S) at 0° and maximum (5.98 km/s in Ka and 7.12 km/s in I/S) at 90°. The variation in the compressional velocity in older Cambay shale for both I/S and Ka is almost the same with the minimum of both being at 40° angle from the bedding plane which is 6.5 km/s in I/S and 6.3 km/s in Ka. The sudden decrease may be due to the presence of the pore water or connate water, where the velocity decreases significantly. Connate water is a liquid that is trapped in the pores of sedimentary rocks as they were deposited. Interstitial water or pore water is defined as the water occupying the spaces between sediment particles. The porosity in older Cambay shale may also be high.

The shear wave velocity for I/S in younger Cambay shale remains almost constant whereas for older Cambay shale the shear velocity increases significantly. This may be due to the presence of carbonates along the bedding plane.

The Shear wave velocity for Ka in younger and older Cambay shale starts decreasing from 1.75 and 4.5 km/s, respectively. The decrease may be the result of increasing clay content and organic matter in both the Shales. For shaly sandstone clay content affects the shear modulus more than bulk modulus. Clean sandstones have much higher shear modulus than do shaly sandstone or shale with same porosity suggesting that grain boundary clays significantly reduce the shear modulus but have very little influence on the bulk modulus (Haw et al. 1986).

Fig. 11 Calculated seismic ΔS -waves velocity for I/S and Ka (younger and older Cambay shale) versus the angle of the bedding plane



Anisotropies (in percent) can be evaluated for the clay mineral components by the following relationship (Melaku 2007):

$$A = 200 \left[\frac{(V_{\max} - V_{\min})}{(V_{\max} + V_{\min})} \right]$$

Thus, Anisotropies in younger and older Cambay shale for I/S and Ka are,

$$A_{YS(I/S)} = 200 \left[\frac{(7.1253 - 6.8335)}{(7.1253 + 6.8335)} \right] = 4.18 \%$$

$$A_{YS(Ka)} = 200 \left[\frac{(5.9864 - 5.6855)}{(5.9864 + 5.6855)} \right] = 5.15 \%$$

$$A_{OS(I/S)} = 200 \left[\frac{(7.322 - 6.4479)}{(7.322 + 6.4479)} \right] = 12.69 \%$$

$$A_{OS(Ka)} = 200 \left[\frac{(7.5523 - 6.3285)}{(7.5523 + 6.3285)} \right] = 17.63 \%$$

The elastic anisotropy is a result of the texture of the sample (Tromans 2011). The average anisotropy in younger Cambay shale is 4.5 % and for older Cambay shale it is approximately 15 % which is significantly high (Franco 2007).

Also the elastic parameters can be evaluated using V_p and V_s values for different minerals. The plots shows the variation of Poisson's ratio, Young's modulus and Bulk modulus with the angle θ from the bedding normal symmetric axis:

From Figs. 12, 13, 14 and 15 it can be inferred that for I/S in younger Cambay shale the Poisson's ratio, Shear modulus, Bulk modulus and Young's modulus remain almost constant with the dipping bed angle having the average values of 0.47, 9.4, 96 and 27.5. For the Kaolinite in younger Cambay Shale, the elastic properties show a slight variation.

In older Cambay shale for both the minerals Illite and Smectite (I/S) and Kaolinite (Ka) there is a large variation

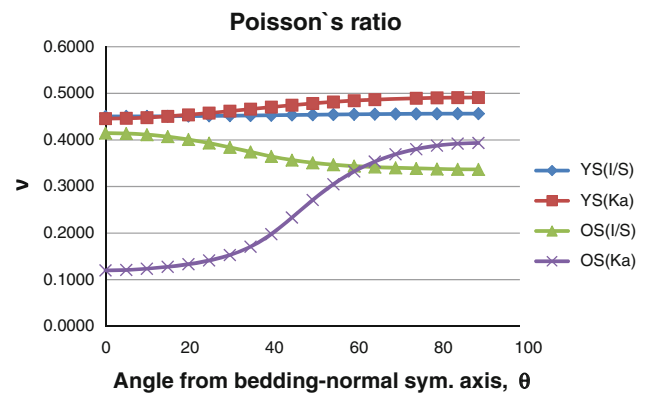


Fig. 12 Poisson's ratio versus θ

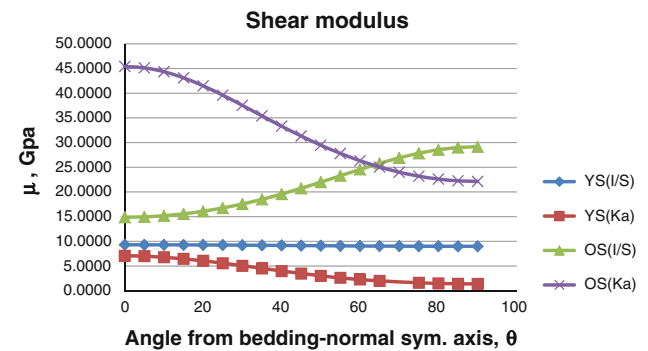


Fig. 13 Shear modulus versus θ

of the elastic properties with the dipping bed. The Shear modulus and Young's modulus show a significant decrease with theta for Kaolinite in older Cambay shale. The Shear modulus of Ka decreases from 45 (0°) to 22.5 (90°) and Young's modulus from 100 (0°) to 60 (90°) whereas the Poisson's ratio and Bulk modulus increase with the increase in dip of the bedding symmetry axis.

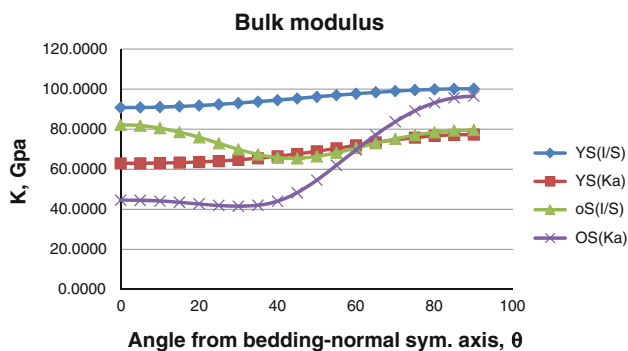


Fig. 14 Bulk modulus versus θ

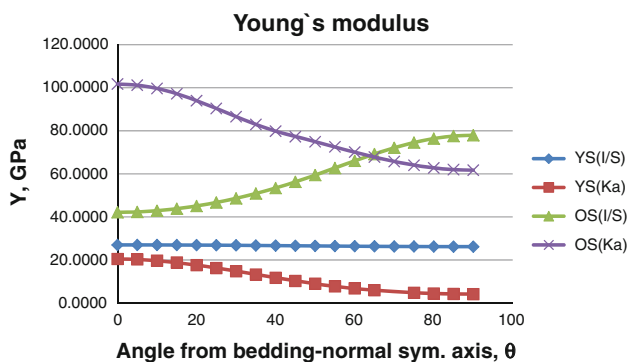


Fig. 15 Young's modulus versus θ

For I/S in older Cambay shale the Shear modulus and Young's modulus show the same increasing trend. The Poisson's ratio decreases with the angle. The Bulk modulus shows a sudden decrease at 40° and then indicates an increasing trend for I/S in older Cambay Shale.

Conclusion

Our study demonstrates the feasibility of extracting orientation distribution of individual component in shales. With the hard X-ray diffraction method and Rietveld method, we are able to quantitatively study the texture of shale and subsequently can calculate the compression and shear velocity with change in angle of the bedding plane. Following observations are obtained from the study:

- The orientation of Ka in older Cambay shale indicates anisotropy.
- Texture strength of Ka is more in younger Cambay shale, whereas I/S has high texture strength in older Cambay shale.
- V_p shows slight variation with the angle of bedding plane which may be due to the presence of low-density material in younger Cambay shale.

- The sudden dip of ΔS at 40° in older Cambay shale may be due to the presence of pore water.
- Anisotropy in older Cambay shale is very high. The Elastic Anisotropy is a result of texture of the sample.
- Anisotropy is more in vertical direction.
- Structure of shale is horizontally foliated.

Open Access This article is distributed under the terms of the Creative Commons Attribution License which permits any use, distribution, and reproduction in any medium, provided the original author(s) and the source are credited.

References

Berryman JG, Grechka V, Berge PA (1997) Analysis of Thomsen parameters for finely-layered VTI media. *Stanford Explor Proj Rep* 94:247–261

Biswas SK (1999) Review of the evolution of rift basins in India during Gondwana with special reference to western Indian basins and their hydrocarbon prospects. *PINSA* 65(A3):226–238

Chowdhary LR (2004) Petroleum geology of the Cambay basin, Gujarat, India. Indian petroleum publishers, Dehradun, pp 74–111

Franco GJ (2007) Seismic anisotropy in tight gas sandstones, Ruli sou field, Piceance basin, Colarado. Msc (Geophysical Engineering) thesis

Haw DH, Nur A, Morgan D (1986) Effects of porosity and clay content on wave velocities in sandstones. *Geophysics* 51(11):2093–2107

Hornby BE, Schwartz LM, Hudson JA (1994) Anisotropic effective-medium modelling of the elastic properties of shales. *Geophysics* 59:485–504

Khan S, Ansari S, Han H, Khosravi N (2011) Importance of shale anisotropy in estimating in situ stresses and wellbore stability analysis in Horn river basin. In: *CSUG/SPE 149433*, presented at the Canadian unconventional resources conference held in Calgary, Alberta, Canada

Lonardelli I, Wenk H-R, Ren Y (2007) Preferred orientation and elastic anisotropy in shales. *Geophysics* 72(2):33–40

Lutterotti L, Matthies S, Wenk H-R, Schultz AS, Richardson JW (1997) Combined texture and structure analysis of deformed limestone from time-of-flight diffraction spectra. *J Appl Phys* 81:594–600

Matties S, Humbert M (1993) The realization of the concept of a geometric mean for calculating physical constants of polycrystalline materials. *Physica Status Solidi B*177:47–50

Melaku MT (2007). Velocity anisotropy of shales and sandstones from core sample and well log on the Norwegian continental shelf. Dissertation, University of Oslo

Pena FR (1998) Elastic Properties of Sedimentary Anisotropic Rocks. Dissertation, Massachusetts Institute of Technology, pp 19–26

Reitveld HM (1969) A profile refinement method for nuclear and magnetic structures. *J Appl Crystallogr* 2(2):65–71

Sandrea R (2012) Evaluating production potential of mature US oil and gas shale plays. *Oil and Gas Journal*, Penwell Publications, USA

Scarrar SC, Ray DS, Kararic AD, Lal NK (2000) Geology, sedimentation and petroleum systems of Cambay basin, India. In: 5th International conference and exposition on petroleum geophysics, New Delhi, pp 215–226

Schoenberg M, Sayers CM (1995) Seismic anisotropy of fractured rock. *Geophysics* 60:204–211

- Sondergeld CH, Rai CS (2011) Elastic anisotropy of shales. *Lead Edge* 30:324–331
- Thomsen L (1986) Weak elastic anisotropy. *Geophysics* 51:1954–1966
- Tromans D (2011) Elastic anisotropy of HCP metal crystals and polycrystals. *IJRRAS* 16(4):462–483
- Wenk H-R, Lonardelli I, Franz H, Nihei K, Nakagwa S (2007) Preferred orientation and elastic anisotropy of illite-rich shale. *Geophysics* 72(2):69–75